In-depth Analysis of Structural Heterogeneity in High Entropy Bulk Metallic Glasses Using 4D-STEM

Minhazul Islam, Ji Young Kim, Geun-Hee Yoo, Soohyun Im, Gabriel Calderon Ortiz, Eun Soo Park, Jinwoo Hwang

Microscopy and Microanalysis, **30** (Suppl 1), 2024, 1359–1360
https://doi.org/10.1093/mam/ozae044.668

Microscopy AND Microanalysis

Meeting-report

In-depth Analysis of Structural Heterogeneity in High Entropy Bulk Metallic Glasses Using 4D-STEM

Minhazul Islam[1], Ji Young Kim[2], Geun-Hee Yoo[2], Soohyun Im[1], Gabriel Calderon Ortiz[1], Eun Soo Park[2], and Jinwoo Hwang[1,*]

[1]*Department of Materials Science and Engineering, The Ohio State University, Columbus, OH, USA*
[2]*Department of Materials Science and Engineering, Seoul National University, South Korea*

*Corresponding author: hwang.458@osu.edu

High-entropy bulk metallic glasses (HE-BMGs) have been recently developed to encompass the characteristics of bulk metallic glasses (BMGs) and high-entropy alloys (HEAs) by substituting the constituent elements with elements that have similar chemical properties in a prototypical BMG. Many of these HE-BMGs, including $Pd_{20}Pt_{20}Ni_{20}Cu_{20}P_{20}$ [1] and $Ti_{20}Zr_{20}Cu_{20}Ni_{20}Be_{20}$ [2], showed superior properties, such as higher glass-forming ability and yield strength, as compared to their conventional BMG counterparts. While these effects are typically attributed to high entropy, the actual effects of configurational entropy on the BMG's properties have been largely unexplored. A more detailed study on the configurational entropy was performed on CuZr-based HE-BMGs [3], where the equiatomic binary $Cu_{50}Zr_{50}$ was systematically expanded to denary $(CuNiBeCoFe)_{50}(ZrTiHfTaNb)_{50}$ HE-BMG while minimizing the effect of the atomic size difference and enthalpy of mixing among the atoms. The results showed that there is a linear change in the mechanical properties measured by nanoindentation (e.g., hardness, (Fig. 1b), while glass-forming ability was at its maximum at the intermediate composition $(CuNiBe)_{50}(ZrTiHf)_{50}$ (Fig. 1a) [3], suggesting a complex relationship between the configuration entropy and the properties.

To help explain the observed behavior, in the present work, the same CuZr-based HE-BMGs were examined using 4D-STEM, followed by the angular correlation (AC) analysis of the 4D-STEM nanodiffraction patterns. This analysis can reveal the details of medium range ordering (MRO) and how it constitutes the structural heterogeneity at the nanometer scale of BMGs that has been shown to correlate to many of their important properties [4]. Individual nanodiffraction patterns from 4D-STEM are transformed to AC functions (Figs. 2a to 2c), which are then Fourier transformed (FT) to reveal the dominant frequency (n) of the constituent sinusoidal functions, which we use as the signature of the rotational symmetry (i.e., n-fold) of the MRO detected at each nanoscale location of the sample (Fig. 2e). Then, the n-fold (e.g., 2-fold) information can be used to reconstruct the real space map of the n-fold that shows the overall size, degree, and locations of the MRO regions [5] that we can compare among different compositions.

The results reveal stark differences among the different compositions. $Cu_{50}Zr_{50}$ showed the distribution of hotspots (Figs. 3b and 3c), which are indicative of MRO regions within the amorphous structure. $(CuNiBe)_{50}(ZrTiHf)_{50}$, showed increased size of the MRO regions and some connection between them (Figs. 3e and 3f), suggesting that the higher glass-forming ability may be related to such changes in MRO. On the other hand, the $(CuNiBeCoFe)_{50}(ZrTiHfTaNb)_{50}$ showed significantly subdued hotspot intensities (Figs. 3h and 3i), suggesting that the degree of MRO in this high entropy composition is substantially less and the structure is much more homogeneous as compared to the others, which is likely correlated to the changes in the mechanical properties measured in nanoindentation. Possible mechanisms for such correlations will be discussed in this presentation [6].

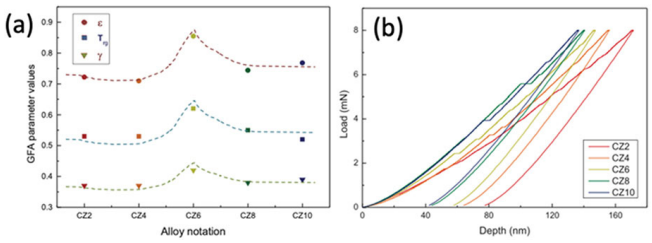

Figure 1. (a) Glass-forming ability and (b) Nanoindentation results from $Cu_{50}Zr_{50}$ (CZ2), $(CuNiBe)_{50}(ZrTiHf)_{50}$ (CZ6), and $(CuNiBeCo\ Fe)_{50}(ZrTiHfTaNb)_{50}$ (CZ10) [3].

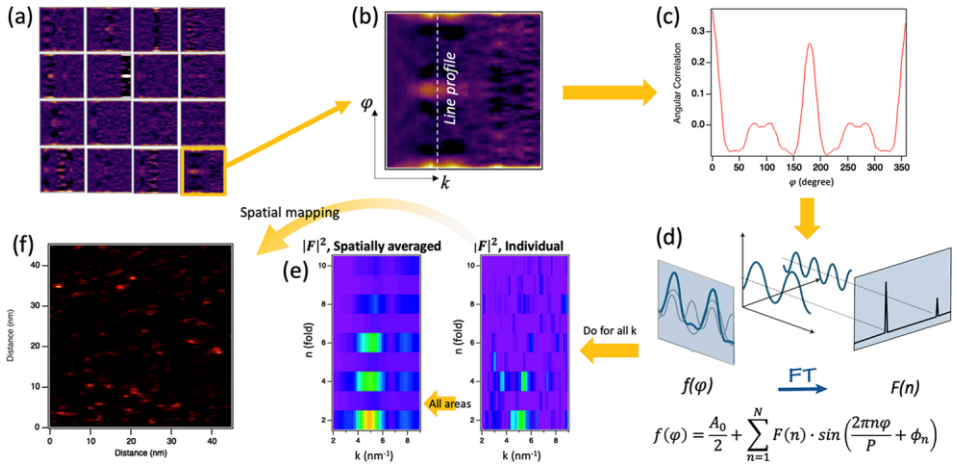

Figure 2. (a) Example AC functions from 4D-STEM. (b to d) FT process that applies for all k in each of the AC functions, which leads to the power spectrum (FT2) as a function of frequency (n) vs. k plot shown in (e). (f) Spatial map of n = 2 reconstructed from the power spectrum data.

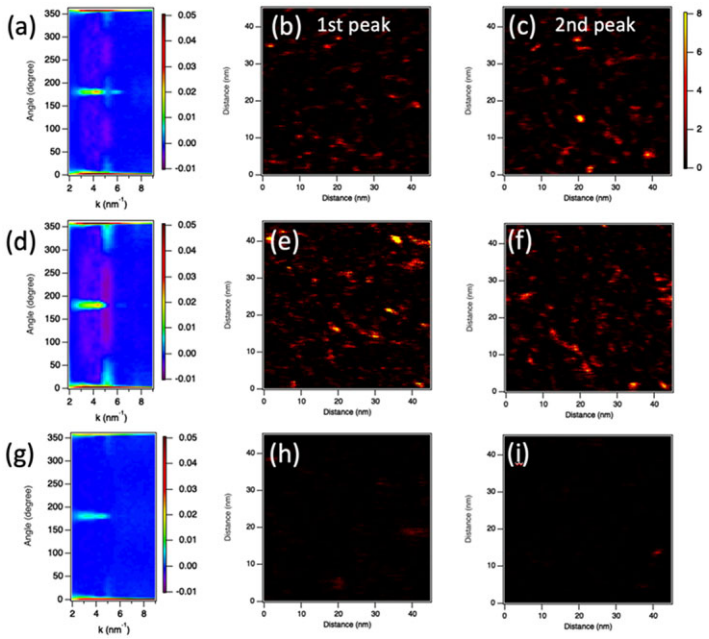

Figure 3. (a) Averaged AC function and (b and c) Real space map of n = 2 for $Cu_{50}Zr_{50}$ for the 1st and 2nd peak location in the AC function for $Cu_{50}Zr_{50}$. (d to f) Same for $(CuNiBe)_{50}(ZrTiHf)_{50}$. (g to i) Same for $(CuNiBeCo\ Fe)_{50}(ZrTiHfTaNb)_{50}$.

References

1. Takeuchi, A., *et al.*, *Intermetallics* **19**, 1546–1554 (2011).
2. Tong, Y., *et al.*, *Journal of Non-Crystalline Solids* **452**, 57–61 (2016).
3. Lee, J. S., *et al.*, *Materialia* **9**, 100505 (2020).
4. Im, S. *et al.*, *Physical Review Materials* **5**, (2021).
5. Im, S., *et al.*, *Ultramicroscopy* **195**, 189–193 (2018).
6. We acknowledge funding support from National Science Foundation, under DMR-2104724.